THE JOURNAL OF BIOLOGICAL CHEMISTRY
Vol. 273, No. 42, Issue of October 16, pp. 27438–27448, 1998
© 1998 by The American Society for Biochemistry and Molecular Biology, Inc.
Printed in U.S.A.

The Dependence of Membrane Permeability by the Antibacterial Peptide Cecropin B and Its Analogs, CB-1 and CB-3, on Liposomes of Different Composition*

(Received for publication, March 10, 1998, and in revised form, July 30, 1998)

Wei Wang, David K. Smith, Keith Moulding, and Hueih Min Chen‡

From the Department of Biochemistry, Hong Kong University of Science and Technology, Clear Water Bay, Kowloon, Hong Kong

A natural antibacterial peptide, cecropin B (CB), and designed analogs, CB-1 and CB-3, were synthesized. The three peptides have different structural characteristics, with CB having one hydrophobic and one amphipathic α-helix, CB-1 having two amphipathic α-helices, and CB-3 having two hydrophobic α-helices. These differences were used as the rationale for a study of their efficacy in breaking liposomes with different combinations of phosphatidic acid and phosphatidylcholine. Biosensor binding measurements and encapsulating dye leakage studies showed that the higher binding affinity of CB and CB-1 to the polar heads of lipids is not necessary for the peptides to be more effective at lysing lipid bilayers, especially when liposomes have a higher phosphatidic acid content. Kinetic studies, by intrinsic and extrinsic fluorescence stopped-flow measurements, revealed two transitional steps in liposome breakage by CB and CB-1, although only one kinetic step was found for CB-3. Circular dichroism stopped-flow measurements, monitoring the formation of secondary structure in the peptides, found one kinetic step for the interaction of all of the peptides with the liposomes. Also, the α-helical motif of the peptides was maintained after interacting with the liposomes. Based on these results, the mechanisms of liposome lysis by CB, CB-1, and CB-3 are discussed.

Antibacterial peptide groups such as the magainins (1), defensins (2), and cecropins (3) are found widely in the animal kingdom. Within each group their sequences are highly conserved and have a high proportion of basic amino acids. Cecropins and magainins have a propensity to form α-helices, and, when helical, these peptides can permeate the lipid bilayer membranes of most Gram-positive and Gram-negative bacteria causing cell death (4, 5), yet they do not affect normal eukaryote cells (4). Unlike melittin (6) or designed amphipathic peptides with the exception of $(KLGKKLG)_3$ (7), the antibacterial magainins and their analogs were also found to be able to lyse hematopoietic tumor and solid tumor cells with little toxic effect on normal blood lymphocytes (5). Thereafter, other antibacterial peptides were found to have similar abilities to kill cancer and/or viral cells (8–10). Based on the findings noted above, these short peptides may be renamed as antibacterial/antimalignant (aBaM)[1] peptides.

Although the mechanisms by which the aBaM peptides cause cell death are not fully understood, it is generally considered that the peptides associate with the membrane and form structural segments that either aggregate and form pores in the membrane or cover the membrane with a detergent-like "carpet" of peptides which then destabilizes the packing of the lipids in the membrane (11–13). Pore formation, a "perpendicular" assembly of the peptides, and the transport of ions as the means of cell death are supported by observations of discrete conductance changes across the membrane (14–16). Recently, the β-sheet-containing defensins and the α-helical peptide, melittin, were shown to form multimeric pores when interacting with lipid bilayers by use of a technique that also allows the size of the pore to be estimated (17, 18). A "parallel" arrangement of peptides on the membrane surface, as an alternative method of cell killing, is suggested by an absence of a membrane potential and the high peptide stoichiometry required for membrane lysis (13, 19).

Because aBaM peptides are capable of lysing a variety of cells but are less effective on other types of cells, understanding the factors behind this variability may lead to the design of viable peptide antibiotics. The initial association of the peptide with the membrane might be an important determinant of the specificity and effectiveness of the peptide. Differences in the construction of the outer leaflet of the cell membrane, such as the lipopolysaccharides found on Gram-negative bacteria, the microvilli on cancer cells (20), or the greater anionic nature of some membranes, such as tumor cells (21), might influence this. It has been shown, for example, that the binding affinity between bactericidal permeability-increasing protein and lipopolysaccharide is a preliminary step to the protein enhancing the permeability of bacteria (22). Microvilli on a cell will increase the surface area of the membrane which can interact with a peptide, and many aBaM peptides have an amphipathic helix with a cationic face that would be expected to interact more efficiently with an anionic membrane. Extensive studies on the role of electrostatic interactions in the binding of cationic, designed peptides and small toxins to anionic lipid bilayers, using both theoretical and experimental approaches, have been undertaken by the Honig and McLaughlin groups (23–26). The significance of the anionic content of the membrane on the

* This work was supported in part by Grant HKUST DAG96/97.SCO2 from the Hong Kong University of Science and Technology. The costs of publication of this article were defrayed in part by the payment of page charges. This article must therefore be hereby marked "*advertisement*" in accordance with 18 U.S.C. Section 1734 solely to indicate this fact.

‡ To whom correspondence should be addressed. Tel: 852-2358-7294; Fax: 852-235-81552; E-mail: bchmc@ust.hk.

[1] The abbreviations used are: aBaM, antibacterial/antimalignant; CB, cecropin B; CB-1, cecropin B-1; CB-3, cecropin B-3; DL, dye leakage; HFP, 1,1,1,3,3,3-hexafluoro-2-propanol; HPLC, high performance liquid chromatography; LUV, large unilamellar vesicle; PA, phosphatidic acid; PBS, phosphate-buffered saline; PC, phosphatidylcholine; RU, resonance signal; SPR, surface plasmon resonance; SUV, small unilamellar vesicle; TEM, transmission electron microscopy; β, fraction of PA (PA/(PA + PC)).

This paper is available on line at http://www.jbc.org

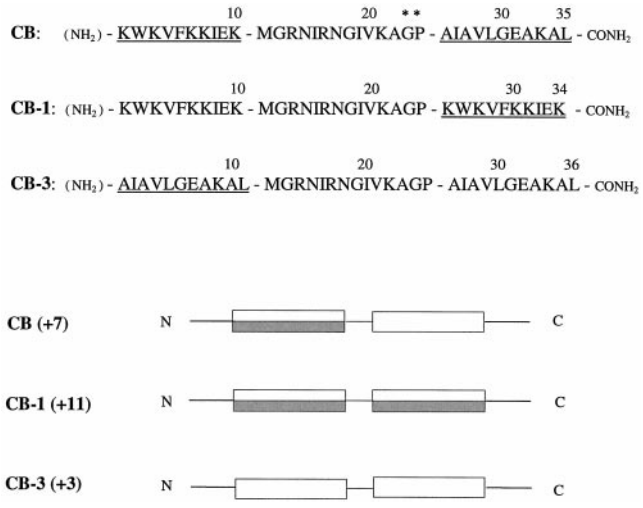

FIG. 1. **Amino acid sequences and structures of CB, CB-1, and CB-3.** In CB, the *underlined* segments indicate the NH_2-terminal amphipathic and COOH-terminal hydrophobic helices. The hinge between the two helices is at Gly^{23}-Pro^{24} (*). In CB-1 the COOH-terminal hydrophobic helix was replaced by the NH_2-terminal amphipathic helix of CB, and in CB-3 the NH_2-terminal helix was replaced by the COOH-terminal hydrophobic helix of CB. The peptide structures are indicated by the diagrams with the net charges of the peptides indicated. Amphipathic and hydrophobic helices are represented by *partly shaded* and *open rectangles*, respectively.

ability of cationic peptides to cause lysis has been demonstrated by White and co-workers in their studies of defensins (17, 27).

The physical nature of the peptide itself may also have an important role. The extent of the cationic charge of the peptide, whether it is amphipathic over its entire length or has amphipathic and hydrophobic segments or if it forms a hinged or continuous structural motif could be factors that influence its efficacy, selectivity, or mode of action. Cecropins, originally isolated from the immune hemolymph of the moth *Hyalophora cecropia* (3, 4, 28), have both antibacterial and anticancer properties (8, 29–32). To date, the three-dimensional structures of three cecropin peptides have been determined. Cecropin A (33) and sarcotoxin IA (34) have a helix-hinge-helix motif, whereas the mammalian cecropin P1 (35) forms a continuous α-helix. The NH_2-terminal helix (or region) is amphipathic with a strongly basic face, and the COOH-terminal helix (or region) is largely hydrophobic.

To investigate further the role of the composition of the membranes and the physical characteristics of aBaM peptides in cell lysis we have studied the action of cecropin B (CB) and two designed analogs on membranes consisting of varying ratios of phosphatidic acid (PA) and phosphatidylcholine (PC). Based on circular dichroism (CD) measurements (32) and sequence comparisons with the cecropins of known structure, CB can be expected to have the helix-hinge-helix motif of cecropin A (33) and sarcotoxin IA (34). The expected NH_2-terminal helix is amphipathic with many lysine residues, the supposed COOH-terminal helix is largely hydrophobic, and a hinge region is expected at Gly^{23}-Pro^{24}. To examine the role of the physical character of the peptide, we constructed two analogs of CB with different properties. CB-1 has two amphipathic helices, and CB-3 has two hydrophobic helices, thereby allowing us to characterize the role of these regions in membrane lysis. The sequences and structures of the peptides are shown in Fig. 1.

We examined the binding of the peptides to lipid bilayers with respect to both the concentration of the peptides and the varying degrees of acidity of the liposomes by means of biosensor measurements. The ability of the peptides to disrupt liposomes was investigated by dye leakage (DL). Finally, kinetic studies based on stopped-flow fluorescence (both tryptophanyl and dye leakage) and stopped-flow CD were used to determine rate constants for the interaction of the peptides with the liposomes. These observations elucidate further the role of membrane composition and the physical character of the peptide in the action of aBaM peptides on membranes and suggest that the mechanisms of liposome lysis by these peptides are also consistent with other observations on channel formation (13, 19, 36) and membrane destabilization (14–16).

EXPERIMENTAL PROCEDURES

Materials

PC was prepared and purified from fresh egg yolk to a purity of approximately 99%. PA was prepared from egg yolk PC using cabbage phospholipase D. The purity of PA was approximately 98%. 1,1,1,3,3,3-Hexafluoro-2-propanol (HFP) and Triton X-100 were purchased from Sigma. The fluorescent dye, calcein (710.5 Da), was a product of Behring Diagnostics. Sodium dodecyl sulfate (SDS) was obtained from Sigma. Isooctane (HPLC grade) was from Fisher Chemical Co. Phosphotungstic acid was a gift from Dr. D. K. Banfield, Department of Biology, Hong Kong University of Science and Technology. The water used for these experiments was deionized and distilled.

Preparation of Vesicles

Small Unilamellar Vesicles (SUVs)—SUV dye-encapsulating (100 mM calcein) liposomes and blank liposomes with different compositions (β = PA/(PA + PC) from 0 to 1) were prepared using a sonicator (Laboratory Supplies Co. model G112 SPIT). Detailed procedures for producing these liposomes have been described elsewhere (32). Liposomes were separated from free (unencapsulated) calcein dye through a Sephadex G-25 column.

Large Unilamellar Vesicles (LUVs)—To produce LUVs for investigation by transmission electron microscopy, liposomes were prepared by an extrusion method. A 20-mg mixture of PA and PC, with β varied from 0 to 1, was dissolved in 1 ml of chloroform. The solvent was then removed by an argon stream. The solute lipid, left on the bottom of the glass tube, was hydrated and dispersed into 2 ml of 10 mM phosphate-buffered saline (PBS) at pH 7.4. The lipid solution was then treated by 10 cycles of freezing in liquid nitrogen and thawing in a 50 °C water bath. The milky solution was extruded, seven times, through 100-nm polycarbonate filters by a LiposoFast extruder (AVESTIN, Inc.). Monolayer lipids were prepared by shaking a mixture of 100 mM SDS (beyond the critical micellar concentration) and 10 mM PBS at pH 7.4 in room temperature. Lipid concentrations were determined using a phospholipid assay reagent (Wako Pure Chemical Industries) in a method based on the Bartlett (37) assay, and the results are expressed in terms of the concentration of phosphorus.

Preparation of Peptides

CB, CB-1, and CB-3 peptides were generated by an Applied Biosystems Inc. 431 peptide synthesizer as described previously (32). The characteristics of another cecropin analog, CB-2, were similar to those of CB-1 (32), and therefore CB-2 was omitted from these experiments. After purification, the peptides were lyophilized. The peptide content was calculated by performing quantitative amino acid analysis with norleucine as an internal reference amino acid, and the purity of the peptide was measured by HPLC. This showed that the purity/peptide content for CB, CB-1, and CB-3 are 95%/71%, 96%/73%, and 95%/76%, respectively. For each peptide the net weight was calculated by multiplying the raw weight by the purity (percent) and peptide content (percent). The concentrations of peptide stock solutions were determined from the net weight of peptides and their molecular weights. Concentrations measured by the above method were confirmed with a bicinchoninic acid assay (Micro BCA protein assay; Pierce Chemical Co.). A negligible deviation between these two methods (less than 6%) was observed.

Transmission Electron Microscopy (TEM)

The liposome specimens for TEM were prepared with a negative stain. A carbon-coated grid was clamped by a pair of forceps with the carbon film face up, and the grid was covered by a drop of 0.4 mM liposomal solution for 1 min. Then, the liquid phase of the liposome drop was drawn off using a wedged filter paper (Whatman no. 1) held perpendicular to the plane of the grid. Before the grid film dried, a drop

of staining solution (2% phosphotungstic acid at pH 7.4) was added. This solution was left for 1 min and then drawn off by a filter paper. The grid containing the liposome sample was dried further in air. TEM investigations were conducted using a JEOL 2010 electron microscope with 0.2-nm resolution. 100-ml mixtures of liposomes ($\beta = 0.25$, 0.4 mM) with CB, CB-1, or CB-3 (20 μM) were incubated for 20 min and then prepared for TEM observations using the same procedure.

CD Measurements

CD spectra of the peptides were measured with a Jasco J-720 spectropolarimeter. Water-jacketed quartz cells with a light path of 1 mm were used. Analysis of CD spectra was done according to the procedure of Chang *et al.* (38). The peptide concentrations were 20 μM with 2.5 μM sodium phosphate buffer, and the pH was adjusted to 6.4. A standard chemical, D-10-camphor sulfonate, at a concentration of 0.06% (w/v in water), in a 1-cm path length cuvette was used for calibration, and the CD was taken as +190.4 millidegrees at 290.5 nm. After the calibration, experiments were conducted at a temperature of 23 °C which was maintained by a circulating water bath. Experiments were repeated at 10 μM for $\beta = 0.25$ and 0.50 and gave results very similar to those with the 20 μM data when a cuvette path length of 2 mm was used.

Binding Analysis by Biosensor

Liposomes with various compositions of PA and PC were prepared by the sonicating method described before. To obtain a lipid monolayer, the liposomes in Dulbecco's phosphate buffer saline (5 mM, 120 μl) were poured into the sensor chip HP A at a flow rate of 2 μl/min. Irregular and loosely bound adsorbents such as multiple lipid layers and unbroken fused liposomes were removed by increasing the flow rate to 100 μl/min for 5 min and then injecting washing solutions such as NaOH or HCl (100 mM) at a flow rate of 10 μl/min for 1 min. The monolayer can be recycled and used for other peptide binding studies by removing the bound peptides with 100 mM NaOH or HCl. 1–2 min was required to wash the peptides from the lipid monolayers. Two steps of injecting 10 μl of 100 mM NaOH followed by 10 μl of 100 mM HCl at a flow rate of 10 μl/min were used. After this process, the base line returned to the level seen before adding the peptides.

Surface plasmon resonance (SPR) detects changes in the refractive index of the surface layer of peptides and lipids in contact with the sensor chip. A sensorgram is obtained by plotting the SPR angle against time. The curve of resonance signal (RU) as a function of time displays the progress of the interaction between the peptides and monolayer lipids at the sensor surface. A standard protein, bovine serum albumin, was used to assess the extent of coverage of the monolayer surface. Association and dissociation rate constants were calculated from the primary sensorgram data by nonlinear fitting (39, 40) using the software supplied by the manufacturer. The dissociation constant, k_d, is derived from the following equation:

$$\ln(S_t/S_0) = -k_d(t - t_0) \quad \text{(Eq. 1)}$$

where S_t is the SPR signal in RU at time t, S_0 is the response at an arbitrary time before the starting time of dissociation, t_0. The association constant, k_a, can then be obtained from the equation:

$$\ln(dS/dt) = -(k_d + k_a\lambda)t + \ln(k_a\lambda S_{\max}) \quad \text{(Eq. 2)}$$

where dS/dT indicates the rate of change of the SPR signal, λ is the concentration of analyte, and $S_{\max}$ is the maximum analyte binding capacity in RU. The Gibbs free energy of ΔG_a was obtained by the following equation (24):

$$(\Delta G_a) = -RT\ln(k_a) \quad \text{(Eq. 3)}$$

where R is the gas constant (1.987 cal K^{-1} mol^{-1}) and k_a is the association constant. This calculation of ΔG_a is based on the simplifying (inaccurate) assumption that there is a one-to-one to association between peptide and lipid (24). Possible differences between the calculations of Ben-Tal *et al.* (24) and the calculations reported here are that Ben-Tal *et al.* assume that the partition constant is a reasonable estimate of the equilibrium association constant, and the association constant calculated here is determined under steady-state conditions.

Dye Leakage Measurements

The lipid concentration used for the experiments was about 2 mM (stock solution). For a typical DL assay, an aliquot of peptides (0.5–6 μM) in PBS buffer was added into the liposome or reversed micellar solution. The solution was incubated for 2 h before fluorescent measurements were conducted. The intensity of fluorescence was measured by a Perkin-Elmer luminescence spectrofluorometer (model LS 50B) with an excitation wavelength of 496 nm and an emission wavelength of 517 nm. The 0% and 100% DL levels were measured as the fluorescence intensity of a vesicle solution including the encapsulated dye without and with Triton X-100 (0.1%), respectively. The percentage of DL induced by a peptide was calculated by the following equation:

$$\mathrm{DL}(\%) = ((F - F_0)/(F_t - F_0)) \times 100 \quad \text{(Eq. 4)}$$

where F is the fluorescence intensity induced by the peptide, and F_0 and F_t represent the intensities at the 0% and 100% DL levels, respectively. Because the different mixing modes of the liposomes and peptides may influence the lipid-breaking process during the DL assays (41) a single peptide stock solution and the same stirring conditions and sample volume were used for each experiment. The experiments were repeated three times, and the results were averaged. If it is assumed that each liposome includes the same amount of encapsulated dye, then DL% will give the percentage of liposmes lysed by the peptides if all of the dye leaks from a liposome. Because the size of the fluorescent dye used in these experiments is about 700 Da, approximately the size of the small dye used by White and co-workers (17), the leakage of dye from the vesicles is likely to be "all-or-none" whether a pore forms or the liposome is destabilized completely (17, 42). Lysis of the liposomes studied here is then defined by the release of the encapsulated dye in an all-or-none manner. However, as shown in our TEM studies (see Fig. 2), liposomes treated with peptides were broken and the resulting pieces aggregated.

Stopped-flow Fluorescence Measurements

A kinetic study of the interactions of peptides and liposomes was conducted using a SX.17MV stopped-flow ASVD spectrofluorometer (Applied Photophysics Ltd., U. K). The nominal mixing time was 2 ms. The system temperature was maintained at 23 °C, which is higher than the lipid phase transition temperature (for lipid egg yolk, its range is between −17 °C and 7 °C). The ratio of liposomes to peptides was 10:1. For intrinsic tryptophan fluorescence measurements, the excitation wavelength was set at 289 nm, and the intensity above 335 nm was recorded as a function of time. For the encapsulated calcein fluorescence experiments, the excitation wavelength was 496 nm, and the emission intensity above 550 nm was recorded. For each experiment, a 121 μM liposome solution was mixed with a 27.5 μM solution of CB, CB-1, or CB-3. The voltage used was 650 V, and 400 data points were collected for each run. Analog signals were converted into digital signals (12 bits), and a nonlinear least square fit was performed with software (Bio sequential SX.17MV) supplied by the manufacturer. This program is based on the Marquardt (43) algorithm. The curve was fitted using the following exponential equation:

$$(F_\infty - F_t)/(F_\infty - F_0) = A_0 + A_1\exp(t/\tau_1) + A_2\exp(t/\tau_2) + A_3\exp(t/\tau_3) \quad \text{(Eq. 5)}$$

where F_∞, F_n, and F_0 are the fluorescence intensity at $t \geq 100$ s, time t, and zero time, respectively. A_i and τ_i are the normalized amplitude and the time constant (or relaxation time) for the ith reaction. The best fit to the number of the exponential terms was determined from the chi square error (44). Measurements were repeated three times at a given condition to ensure reproducibility.

Stopped-flow CD Measurements

A kinetic study of the peptide secondary structural change induced by the interactions with the liposomes (at $\beta = 0.25$) was performed using a SX.17MV stopped-flow ASVD spectrofluorometer. The instrumentation setup was similar to that for the stopped-flow fluorescence measurements; but instead of fluorescence, the probe is CD. The temperature was maintained at 23 °C; the mixing ratio, by volume, was set at 10 (1.3 mM liposome solution) to 1 (25 μM peptide solution). Analog CD signals were recorded at 222 nm and then converted into digital signals (12 bits) before nonlinear least square fitting (as described above) was performed. Measurements were repeated three times at a given condition to ensure reproducibility.

RESULTS

TEM Morphological Observations of Liposomes Affected by CB, CB-1, and CB-3—To confirm the existence and observe the morphology of liposomes, with or without peptides, negative stain TEM was used. The complete shape of the liposomes could be observed with the boundary of the vesicles clearly distinguishable from the gray staining solution. Typical TEM micrographs for liposomes (with $\beta = 0.25$) with and without

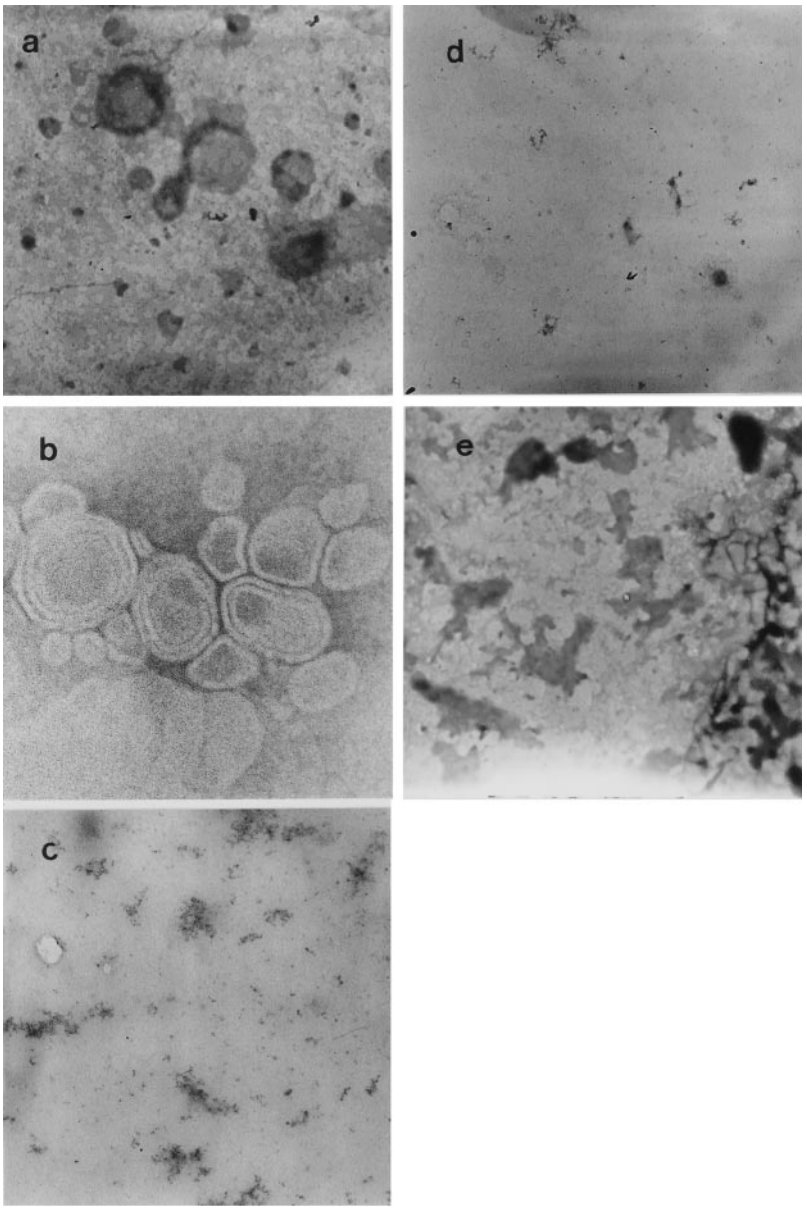

FIG. 2. **Negative stain TEM.** Micrographs of liposomes (with $\beta = 0.25$) are shown with or without peptides. *Panel a*, liposomes without peptide. Liposomes with characteristic circular or elliptical shapes are observed. The largest diameter of these liposomes is about 250 nm. *Panel b*, liposomes without peptide at higher magnification. Some multilayers liposomes can be observed. *Panels c* and *d*, liposomes with CB and CB-1, respectively. Pieces of broken liposome fragments are seen. *Panel e*, liposomes with CB-3. Broken liposomes with irregular shapes are observed.

peptides are shown in Fig. 2. Fig. 2*a* shows the liposomes in the absence of peptides, and they have an elliptical or circular shape. The largest diameter of the liposomes is about 250 nm. When the magnification was enhanced, a small percentage of multilayer liposomes was observed as shown in Fig. 2*b*. When peptides CB and CB-1 were added (20 μM), the circular or elliptical shapes of the intact liposomes became rare, and broken liposome predominated. The resulting broken liposome pieces aggregated, as shown in Fig. 2, *c* and *d*, for CB and CB-1, respectively. This demonstrates that liposomes can be severely disrupted by CB and CB-1. Irregularly shaped broken liposomes were observed after treatment with CB-3 (Fig. 2*e*).

Secondary Structures of CB, CB-1, and CB-3 in SUV Bilayers and SDS Monolayers by CD—The structures of the peptides CB, CB-1, and CB-3 in water are random coils (32). However, α-helical structures formed if lipid vesicles were involved (*32*). These results show that the peptides form α-helices as they approach a polar environment with the backbone hydrogen bonding removing the unfavorable interaction of the peptide bond with a hydrophobic environment (*45*). The secondary structure of the peptides in the presence of SUVs was investigated, and typical CD curves for the peptides with SUVs of $\beta = 0.25$ and $\beta = 0.50$ are shown in Fig. 3, *a* and *b*, respectively. From the CD it can be determined that the α-helical contents of CB, CB-1, and CB-3 at $\beta = 0.25$ and 0.50 are 65.9, 62.8, and 27.3% and 65.7, 54.0, and 58.0%, respectively. CB and CB-1 show similar levels of secondary structure at these β values, whereas CB-3 showed a different effect. At $\beta = 0.25$ the level of secondary structure in CB-3 was reduced, but a higher level was observed at $\beta = 0.50$. This greater formation of secondary structure at higher levels of β might correlate with the greater efficacy of CB-3 on liposomes with higher β values (see below). On liposomes containing other compositions ($\beta = 0.15$ and 0.75), all three peptides showed an α-helical structure (*e.g.* $\beta = 0.15$, CB, 60.4%; CB-1, 59.1%; CB-3, 11.0%; $\beta = 0.75$, CB, 42.5%; CB-1, 46.7%; CB-3, 59.6%). Monolayer experiments are undertaken using SDS lipids, and the CD spectra of peptides on SDS monolayers are shown in Fig. 3*c*. The helical contents of CB, CB-1, and CB-3 were 58.7, 60.9, and 44.6%, respectively. The secondary structure of peptides on monolayers seems more close to those on bilayers with higher content of acidic lipids (compare Fig. 3, *a* and *b*, with *c*). This may reflect the similar charged environment for bilayers lipids with higher β and the anionic (net charge –1) SDS monolayer. However, the differ-

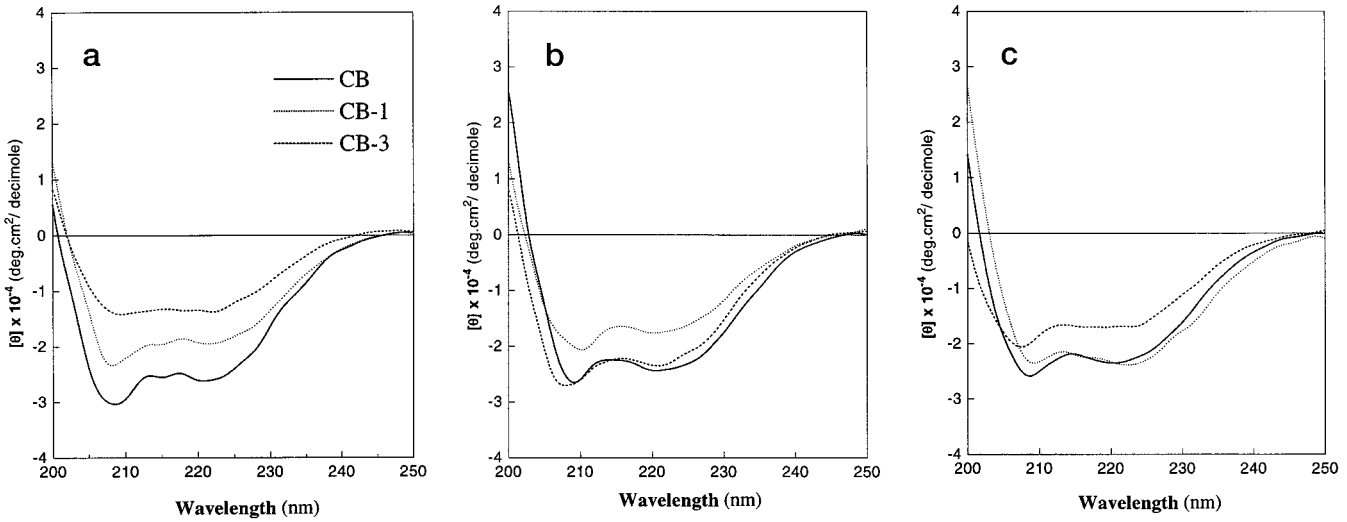

FIG. 3. **CD spectra of peptides.** *Panel a*, on SUVs at $\beta = 0.25$. *Panel b*, on SUVs at $\beta = 0.5$. *Panel c*, on SDS monolayer micelles.

ences in the CD spectra (Fig. 3*b* shows CB-1 having lower helicity than CB-3, whereas Fig. 3*c* shows CB-3 having the least helicity) may indicate that there is not a direct relationship between the actions of the peptides on bilayers and monolayers.

Binding Affinity of CB, CB-1, and CB-3 on Lipid Monolayers of Different Compositions by SPR—Different mixtures of lipid monolayers, with β ranging from 0 to 0.75, were generated and adsorbed onto the sensor chip HPA. Typical sensorgrams of the bimolecular bindings between the peptides and lipid monolayers (at $\beta = 0.25$) are shown in Fig. 4, *a*, *b*, and *c*, for CB, CB-1, and CB-3, respectively. A series of concentrations (2, 4, 8, and 10 μM) of peptides CB and CB-1 was used (Fig. 4, *a* and *b*), and RU signal intensity increased as the peptide concentration increased. This indicates that the amount of peptide bound to the lipids is proportional to the increase in the peptide concentration. Fig. 4*c* shows that there was no binding between CB-3 and the lipid monolayers because the level of RU for association (*rising curve*) is equal to that for dissociation (*falling curve*). Similar results were obtained for CB-3 from lipid monolayers constructed with other values of β. Sensorgrams indicating the binding relationship between peptides and lipid monolayers constructed with β varying from 0 to 0.75 are shown in Fig. 5, *a* and *b*, for CB and CB-1, respectively. The binding capacity of both peptides increased as the content of PA in the lipid increased, as shown by the higher RU level.

The binding constants of association (k_a) were determined by nonlinear fitting to the primary sensorgram data (Fig. 5). Table I gives the values of k_a for CB and CB-1 interacting with lipids where β ranges from 0 to 0.75. Standard Gibbs free energies of binding (ΔG^o) based on the assumptions of the models of Honig and co-workers (24, 25) were calculated from the apparent association constant and are also shown in Table I. When compared with their experimental results and theoretical calculations (24, 25) based on the application of the Poisson-Boltzmann equation (46) we found that the free energy of binding was somewhat smaller on a per net charge basis, with a slight increase for the more cationic CB-1 (Table I). When the anionic content of the membrane increased, there was also an increase of about 20% in the binding free energy. The similar binding capacity for CB and CB-1 on lipid monolayers with $\beta = 0$ and $\beta = 0.25$ (Fig. 5) may result from the contribution to binding from the polar nature of the lipid heads being close to that from liposomes with small amounts of charged lipids. CB-1 would bind more strongly (Fig. 5*b*) because of its higher cationic content. Because the CD spectra of CB and CB-1 associated with liposomes at $\beta = 0.25$ and 0.5 (see Fig. 3, *a* and *b*, respectively) show that the peptide conformation does not change significantly, the increase in binding from $\beta = 0.25$ (Fig. 5) onward is most likely caused by peptide aggregation.

Efficiency of Lipid Bilayer Lysis by CB, CB-1, and CB-3 on Liposomes of Different Composition as Measured by Dye Leakage—Bilayer lysis by all of the peptides on neutral liposomes, those constructed with PC only, was negligible (data not shown). However, when liposomes contained PA, DL from the liposomes was detected. Fig. 6*a* shows the DL from liposomes (with $\beta = 0.15$) induced by concentrations of the peptides from 0.1 to 6.0 μM. Throughout Fig. 6, CB is represented by *filled circles*, CB-1 by *open circles*, and CB-3 by *filled triangles*. The activity of liposome lysis of CB and CB-1 caused 100% DL at concentrations of 1 μM and 1.5 μM, respectively. However, negligible DL was observed for CB-3. As the content of PA in the liposomes was increased the relative abilities of the peptides to induce DL altered. DL began to be observed for CB-3 at a β level of 0.18 (Fig. 6*b*), and DL increased further at $\beta = 0.22$ (Fig. 6*c*). At these levels CB still reached a 100% DL level but with a higher concentration of peptide required (2.5 μM), and the maximal level of DL caused by CB-1 started to decrease. When β was 0.25 (Fig. 6*d*) CB caused 100% DL at 2.5 μM; and CB-1, although still showing a DL pattern similar to that of CB, reached a plateau of about 80% DL at 2 μM. CB-3 was now more able to cause DL and reached the level achieved by CB-1 when the CB-3 concentration was 6 μM. At a β value of 0.5, CB-3 became the most effective peptide at causing DL from the liposomes, whereas CB and CB-1 showed a similar pattern of effectiveness with CB still slightly more efficient (Fig. 6*e*). When the liposomes had a β value of 0.6 (Fig. 6*f*) CB-1 became marginally more effective than CB at causing DL, although both were considerably less efficient than CB-3, which reached its maximum effectiveness at a concentration of 5 μM. Fig. 6*g* shows the highest level of β examined, and CB-3 causes 100% DL at a concentration of 2.5 μM and is much more effective than CB-1, which is slightly more effective than CB.

The effect of the peptides in this experiment is summarized in Fig. 6*h*, which shows the concentration of peptide required to achieve a DL of 50% (DL_{50}) for each value of β. It can be seen that CB and CB-1 exhibit a similar pattern with the DL_{50} increasing as β increases. CB-3 shows the opposite effect, being most efficient at liposome lysis at the highest β level and also having a much smaller range of DL_{50} values than CB and CB-1. The peptides have approximately equal DL_{50} values when β is 0.5. Another summary of this experiment is provided by the

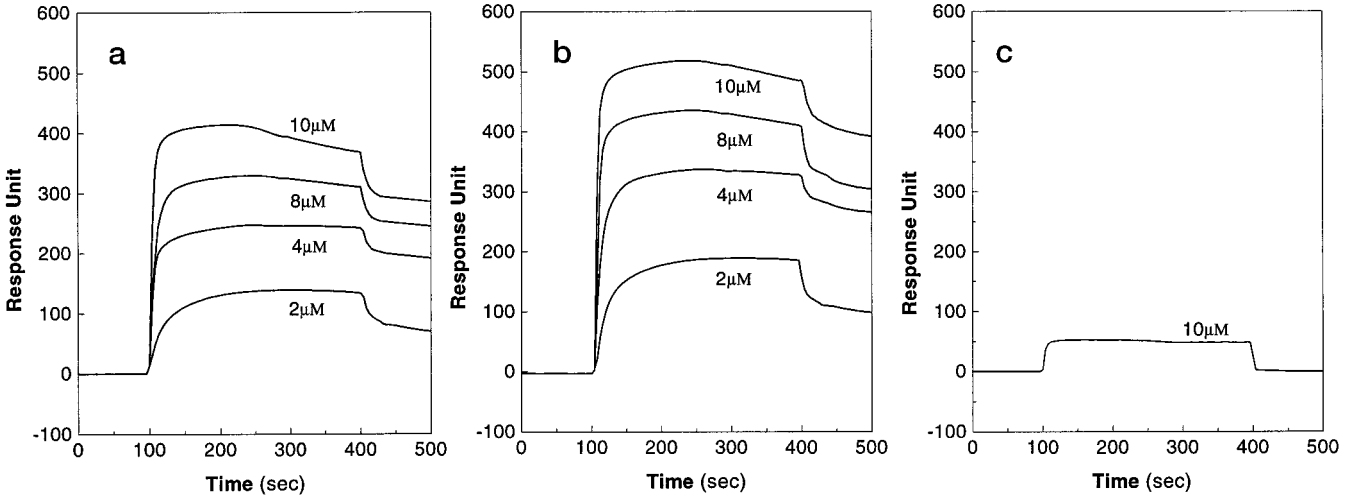

FIG. 4. **Sensorgrams of the binding between various concentrations of the peptides and monolayer lipids with $\beta = 0.25$.** *Panels a* and *b*, CB and CB-1 (respectively) at concentrations of 2, 4, 8, and 10 μM, showing the increase in binding as the peptide concentration increases. *Panel c*, the negligible binding of CB-3 to the monolayer lipids.

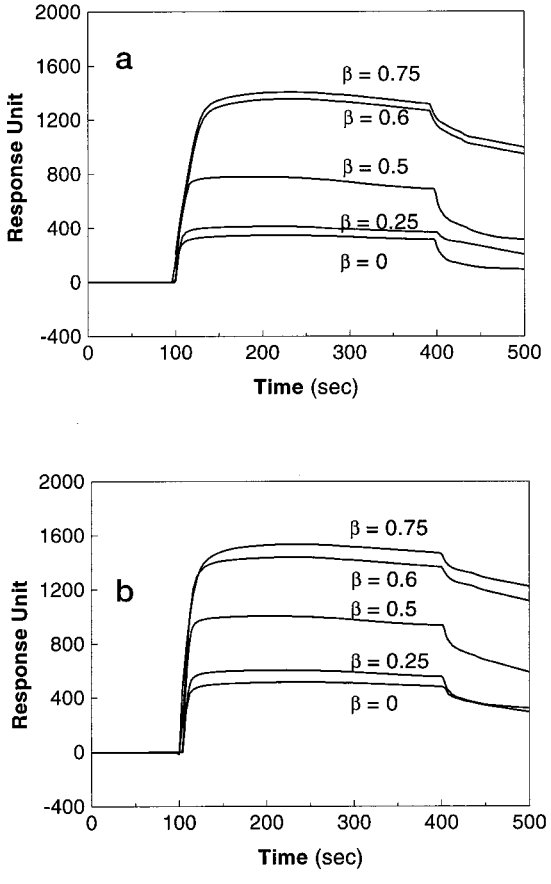

FIG. 5. **Sensorgrams of the binding between peptides and monolayer lipids of varying compositions.** Plots of RU *versus* time for the binding of CB (*panel a*) and CB-1 (*panel b*) at 10 μM to liposomes with $\beta = 0$, 0.25, 0.5, 0.6, and 0.75.

TABLE I

Binding constants of association (k_a) and binding free energies of association (ΔG_a) for peptides, CB, and CB-1, with monolayer lipids of different composition

The temperature was 25 °C, and the peptide concentration was 10 μM. The uncertainty in these experiments was less than 10%.

β	CB		CB-1	
	k_a	ΔG_a	k_a	ΔG_a
	$M^{-1}\,s^{-1} \times 10^4$	*kcal/mol*	$M^{-1}\,s^{-1} \times 10^4$	*kcal/mol*
0.00	0.82	−5.32	0.89	−5.38
0.25	1.32	−5.62	1.52	−5.70
0.50	1.78	−5.80	1.81	−5.81
0.60	1.98	−5.86	2.07	−5.88
0.75	2.64	−6.03	3.04	−6.11

plot of the concentration at which maximal DL was obtained for each of the peptides at each β level (Fig. 6*i*). It should be noted that the maximal DL level achieved was often not the same for the different peptides at a given β level nor for a given peptide at different β levels. As in Fig. 6*h* both CB and CB-1 show similar trends with the concentration of peptide increasing steadily to achieve (a reducing) maximal DL level. Again, CB-3 shows the opposite trend with respect to both concentration and DL level.

Kinetic Study of the Interactions of CB with Liposomes (without Encapsulated Dye) by Fluorescence Stopped-flow Measurements—Because CB possesses only one Trp residue, at position 2 in the NH_2-terminal amphipathic α-helix (see Fig. 1), the change in the microenvironment of this region of the peptide can be monitored during the peptide's interaction with a liposome. If the fluorescent intensity is enhanced, the Trp residue is in a more hydrophobic environment (41). Fig. 7 shows the fluorescence intensity changing as a function of time for the interaction of CB with liposomes of various compositions (β ranging from 0.15 to 0.75). Fluorescence intensity increased with the increase of PA in the liposomes, implying that the Trp of CB tends to be in a more hydrophobic environment in liposomes that contain more PA. Based on the best fit to the data (*solid lines* shown in Fig. 7), two rate constants (τ_i) were obtained for the reaction of CB with liposomes of different compositions and are given in Table II. There are two steps or transition periods (τ_1, τ_2) through the complete reaction between CB and liposomes. As the PA content of the liposomes increased, the time constants of τ_1 and τ_2 became smaller (except for τ_1 at $\beta = 0.75$). This implies that the effectiveness of the association of the peptides with the lipid bilayers is enhanced by the increasing content of PA. In this experiment, neither CB-1 nor CB-3 was used because the former has two tryptophans (positions 2 and 26), and the latter has none.

Kinetic Study of the Interactions of CB, CB-1, and CB-3 with Dye-encapsulating Liposomes by Fluorescence Stopped-flow Measurements—Fluorescence measurements were on calcein-encapsulating liposomes with the extrinsic fluorescence of the

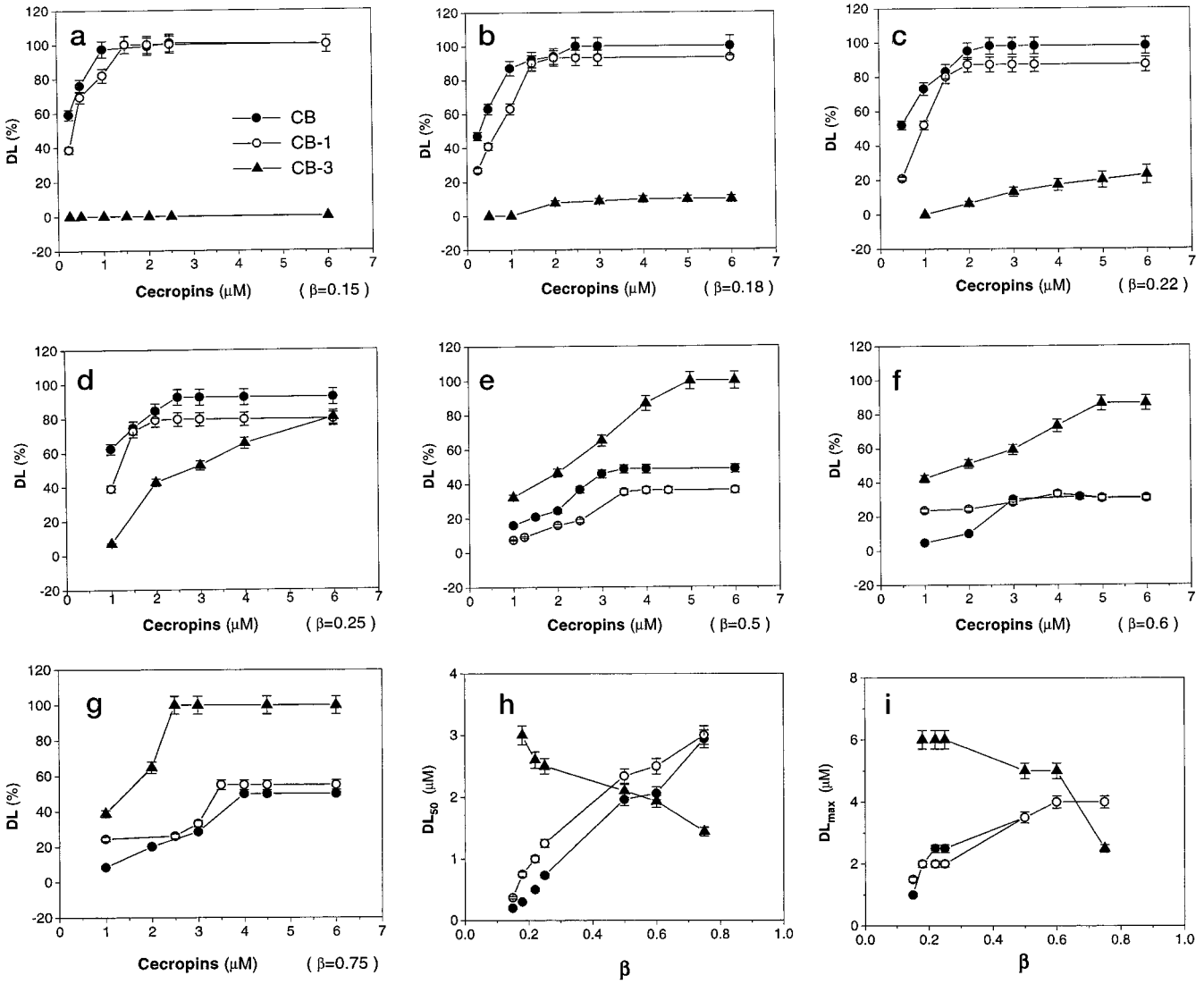

FIG. 6. **Liposome DL measurements.** Percentage dye leakage, DL(%), for CB (*filled circles*), CB-1 (*open circles*), and CB-3 (*filled triangles*) acting on liposomes with $\beta = 0.15$ (*panel a*), 0.18 (*panel b*), 0.22 (*panel c*), 0.25 (*panel d*), 0.50 (*panel e*), 0.60 (*panel f*), and 0.75 (*panel g*). The DL_{50} (*panel h*) and the DL_{max} (*panel i*) values of CB, CB-1, and CB-3 are shown at different liposome β values.

dyes being traced as a function of time as the liposomes were broken down by the peptides. Experiments were performed on liposomes with β at 0.25 and 0.5, and typical examples of the fluorescence intensity change as a function of time for CB, CB-1 and CB-3, acting on the liposomes with β at 0.25, are shown in Fig. 8, *a*, *b*, and *c*, respectively. CB caused the largest amount of dye to be released as shown by the largest change in fluorescent intensity among the three peptides (Fig. 8*a*). CB-1 had the fastest reaction rate (Fig. 8*b*), and CB-3 caused the least change in fluorescence intensity and had the slowest reaction rate. The time constants were determined from a best fit to the fluorescent curves for CB, CB-1, and CB-3 and the values, averaged over three experiments, are presented in Table III. Two kinetic steps were observed for CB and CB-1, whereas only one kinetic step was determined for CB-3.

Kinetic Study of the Interactions of CB, CB-1 and CB-3 with Liposomes by CD Stopped-flow Measurements—Figs. 9, *a*, *b*, and *c* show the CD intensity change as a function of time for CB, CB-1, and CB-3, respectively, interacting with liposomes at $\beta = 0.25$ (note the shorter time scale in Fig. 9*b*). All of the CD signals increased after the peptides interacted with the liposomes. From the best fit to the data, only one kinetic step was obtained, with the time constants being 1.27, 0.15, and 7.70 s for CB, CB-1, and CB-3, respectively. The uncertainty in the CD kinetics was ± 15%. CB-1, the peptide with the highest positive charge, has the fastest rate constant among the three. In contrast, CB-3, which has the least positive charge, has the slowest rate constant. Furthermore, we observed that the secondary structure of the peptides formed during the liposome breaking action and was maintained after liposome lysis.

DISCUSSION

The efficacy of CB, CB-1, and CB-3 on liposomes and their helical content in a hydrophobic environment were confirmed by morphological studies by TEM and by CD. From Fig. 2 it can be seen that both CB and CB-1 lyse liposomes with a PA content of 25% ($\beta = 0.25$) in a similar manner, whereas CB-3 has a different effect when producing broken liposomes. In the presence of liposomes all of the peptides were able to form a helical structure. Secondary structure was observed in the peptides when interacting with liposomes that had β values ranging from 0.15 to 0.75. Fig. 3, *a* and *b*, shows the CD spectra at $\beta = 0.25$ and 0.5, respectively. Whereas CB and CB-1 show fairly consistent levels of helical content, CB-3 has a somewhat lower helical content at lower β levels that might be associated with its lower efficacy on less anionic liposomes. The ability to

form a helical structure in the more hydrophobic environment of the membrane surface, probably influenced by the removal of unfavorable interactions from the peptide bond (45), is considered to be the first stage in the action of aBaM peptides on microbial cells (11). Because all of the peptides had a generally similar helical content it appears that the secondary structural content of the peptides, although necessary, is largely independent of their efficiency in disrupting liposomes. Therefore, the particular sequences and physical characteristics of the peptides may be factors that influence this, and the compositions of the natural and designed peptides used here address this issue.

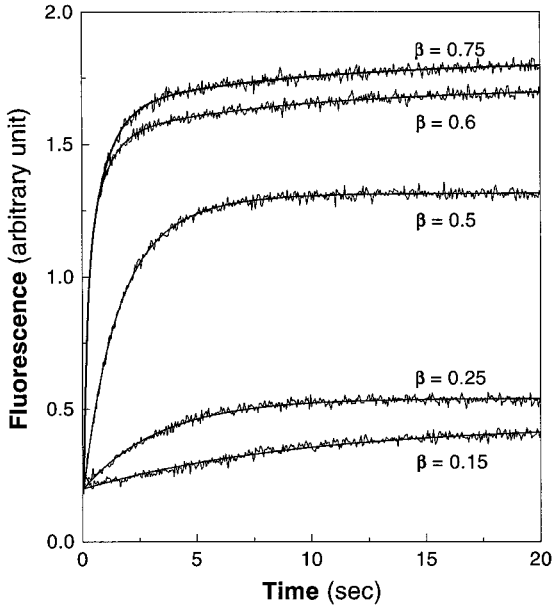

FIG. 7. **Kinetic studies of CB on liposomes by tryptophanyl fluorescence stopped-flow measurements.** The fluorescence intensity change as a function of time after CB was added to liposomes with $\beta = 0.15$, 0.25, 0.5, 0.6, and 0.75. The *spiky curves* are the experimental data, and the *solid lines* represent the best fit to the data using Equation 5 from "Experimental Procecures."

TABLE II
Rate constants from fluorescence of Trp-2 in CB
The uncertainty in these experiments was ±10%.

β	τ_1	τ_2
	s	*s*
0.15	6.30	10.40
0.25	2.18	5.73
0.50	1.26	4.60
0.60	0.29	3.96
0.75	0.33	3.19

An interaction between the cationic face of aBaM peptides and anionic lipids will attract and hold the peptides to the cell surface so they can interact with the lipid. Based on the theoretical studies of small poly-lysine peptides on anionic membranes by Ben-Tal *et al.* (24), it might be expected that the peptides would initially align parallel to the membrane, separated by a few angstroms. This charge interaction might also explain the activity of aBaM peptides on tumor cells, which have more anionic membranes than normal eukaryotic cells (21, 31, 32). The binding studies, using a biosensor, undertaken in this work showed that the cationic peptides, CB and CB-1, bound effectively to the liposomes (at $\beta = 0.25$), with the number of peptides bound increasing with the concentration of the peptide (Fig. 4, *a* and *b*). CB-1, which has a greater number of basic residues (net charge 11+), bound more effectively to the liposomes than CB (net charge 7+), consistent with results from poly-lysine peptides (*24*). However, the mainly hydrophobic CB-3 (net charge 3+) did not show any binding to the liposomes (Fig. 4*c*). When the concentration of PA in the liposomes was varied (β ranging from 0 to 0.75) CB and CB-1 both showed increased binding as the acidity of the liposome increased (Fig. 5, *a* and *b*) in a manner similar to that seen for pentalysine (24). Again, the binding of CB-3 was negligible. Thus, the increasing basic nature of the peptide and the increasing acidity of the lipid enhance the interaction between peptide and lipid. Although CB-3 did not bind to the monolayer lipids in the biosensor experiments it was able to lyse liposomes (Fig. 6). Its association with the lipids is probably driven by hydrophobic interactions causing it to partition from the solvent to the lipid phase where it forms a helical structure (Fig. 3). The peptide might be driven to cluster onto regions of the liposome where neutral lipids predominate. This association would be unlikely under the flow conditions of biosensor measurements. An interaction between the hydrophobic peptide and the hydrophobic lipid tails is probably the path to lipid lysis.

The binding conditions between the peptides and a lipid monolayer fixed to a biosensor chip surface are similar to those

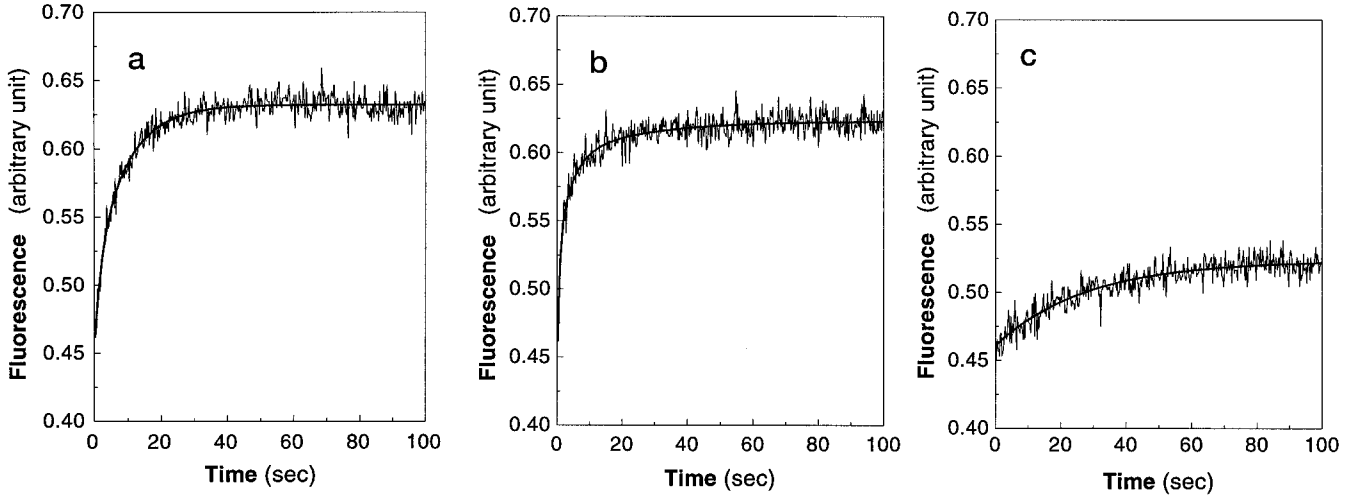

FIG. 8. **Kinetic studies of CB, CB-1, and CB-3 on liposomes by dye-encapsulating fluorescence stopped-flow measurements.** Plots of the fluorescence intensity change as a function of time after CB (*panel a*), CB-1 (*panel b*), and CB-3 (*panel c*) were added to liposomes at $\beta = 0.25$.The *spiky curves* are the experimental data, and the *solid lines* represent the best fit to the data using Equation 5 from "Experimental Procedures."

assumed by Ben-Tal *et al.* (24, 25) in their models in that they assume that the structure of bilayers does not change when peptides or proteins bind. For CB and CB-1 the binding free energy (ΔG_a°) ranges from ~−5.3 to −6.1 kcal/mol as β increases from 0 to 0.75 (Table I). CB-1 has a slightly larger free energy than CB for each β value probably because of the greater net positive charge of CB-1, but it does not show the clear, linear relationship seen in poly-lysine peptides (24). This is likely the result of more complicated interactions of CB and CB-1 with the lipids because of their helical tertiary structure, the steady state (non-equilibrium) binding due to the operation of biosensor, and interactions with the fixed monolayers rather than free lipids may also influence the apparent binding energy. Furthermore, the assumption of one-to-one binding of peptide and lipid for the calculation of ΔG^{o} (24) will be more inaccurate for larger peptides such as CB and CB-1.

DL studies of the efficiency with which the peptides can disrupt liposomes of varying β levels showed interesting trends as β increased. At low levels of β, CB was most effective, with CB-1 nearly as effective, at disrupting the liposomes to release dye (Fig. 6, *a–d*). CB-3 was considerably less effective. As the acidic content of the liposomes increased, however, the efficiency of CB and CB-1 decreased while that of CB-3 increased, so that at a β value of 0.5 and above CB-3 was the most efficient at causing dye leakage from liposomes (Fig. 6, *e–g*). CB and CB-1 showed nearly similar, decreasing efficiencies as β increased, with CB-1 eventually becoming marginally more effective than CB. The general increase in efficiency of CB-3 and the decrease in the efficiency of CB and CB-1 are indicated by the plot of DL_{50} and DL_{max} against β in Fig. 6, *h* and *i*, respectively. This trend in the efficacy of liposome disruption is opposite to that of binding efficiency. As the peptides CB and CB-1 bind more effectively to the more acidic lipids their ability to lyse them decreases. The greater efficiency of CB-3 on acidic liposomes might be caused by the largely nonpolar CB-3 being driven to accumulate on the regions of the lipid where PC dominates. It may then reach a sufficient concentration on the lipid to disrupt the membrane and cause lysis in a cooperative manner, similar to that proposed for cecropin P1 (12). When β is lower, CB-3 might disperse more widely over the membrane and not reach a critical concentration on the membrane at lower solution concentrations of peptide. This is suggested by the results on liposomes at $\beta = 0.25$ (Fig. 6*d*) where a much greater concentration of CB-3, than either CB or CB-1, is required to cause DL. These results imply that the initial binding step, driven by electrostatic interactions, may not be critical for the subsequent action of liposome lysis especially as the acid content of the liposome increases. Stronger binding to the lipid head groups may retain the peptide on the lipid surface and inhibit its ability to enter the bilayer and initiate lysis, or it may assist in forming unproductive aggregates of peptides on the lipid surface. Efficient lysis of lipid bilayers by peptides may not require strong binding energy but a strong perturbing energy in which the structural characteristics of the peptides and other factors may dominate the electrostatic interactions. Further experiments are currently being undertaken in our laboratory to identify these factors.

TABLE III
Rate constants from dye fluorescence measurements

β	0.25		0.50	
	τ_1	τ_2	τ_1	τ_2
CB	2.00 ± 0.20	9.60 ± 1.00	0.66 ± 0.04	14.79 ± 1.10
CB-1	0.86 ± 0.08	6.12 ± 0.60	0.56 ± 0.04	4.86 ± 0.40
CB-3	27.82 ± 3.20		8.62 ± 0.70	

Because CB has a single Trp residue, located in the NH_2-terminal amphipathic helix at position 2, the environment of this residue can be monitored by stopped-flow fluorescence measurements. The change in the fluorescence intensity of Trp[2] over the time course of the experiment is shown in Fig. 7 on liposomes with increasing levels of β. The fluorescence intensity increases rapidly as the peptide associates with the liposome, showing that the Trp residue is in a more hydrophobic environment. As the level of β in the liposomes increases so does the fluorescent intensity. This is consistent with the biosensor binding studies (Figs. 4 and 5) which showed higher affinity binding as β increased. When the peptide associates with the membrane and forms a helix and starts to integrate

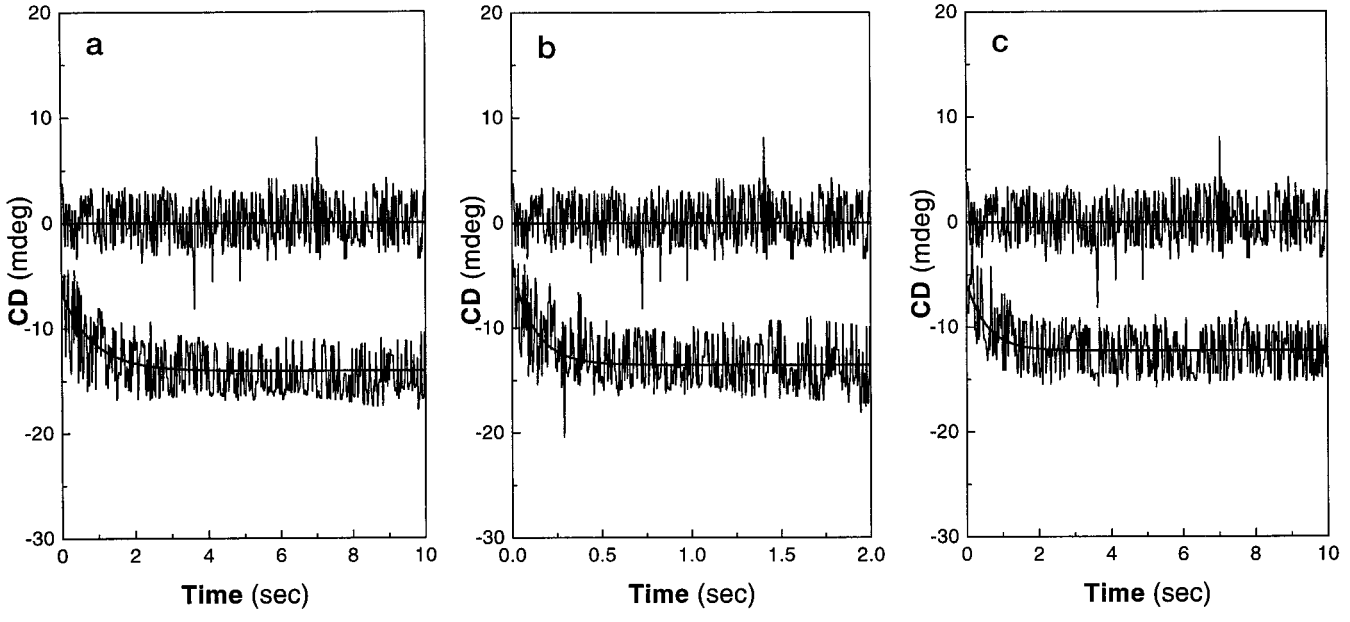

FIG. 9. **Kinetic studies of CB, CB-1, and CB-3 on liposomes by CD stopped-flow measurements.** Plots of the CD intensity change as a function of time after CB (*panel a*), CB-1 (*panel b*), and CB-3 (*panel c*) were added to liposomes with $\beta = 0.25$. The *flat curves* are measurements of the liposome before the peptides were added. The CD intensity increased with time after the peptides were added to the liposomes. The *spiky curves* are the experimental data, and the *solid lines* represent the best fit to the data using Equation 5 from "Experimental Procedures."

into the membrane, the Trp residue becomes protected from the hydrophilic environment. Two rate constants for the reaction were determined for each level of β (Table II), showing a trend to faster rate constants as β increases. The more rapid initial rate constant (τ_1) corresponds to the initial association of the peptide with the membrane, and the slower second rate constant would correspond to a greater integration of the peptide into the hydrophobic bilayer of the membrane (47).

A second stopped-flow fluorescence study of all three peptides interacting with liposomes at β values of 0.25 (Fig. 8) and 0.5 was also conducted (Table III). CB was most effective, followed by CB-1, at causing DL at $\beta = 0.25$ (Fig. 8) consistent with the earlier results (Fig. 6*d*). From these measurements, two rate constants were determined for the interaction of CB and CB-1 with the dye-encapsulating liposomes, but only one for CB-3 (Table III). The two rate constants for CB and CB-1 suggest a two-stage process of an initial association and entry of the peptides into the membrane, which is assisted by the binding affinity of the peptides to the membrane, and a second stage of membrane destruction. This is supportive of a mechanism of pore formation (14–16) as the means of cell destruction. The faster τ_1 rate at $\beta = 0.5$ corresponds to the increase in binding affinity as β increases (Figs. 4 and 5); the slower τ_2 for CB, and approximately equal value for CB-1, corresponds to their reduced efficiency on liposomes as β increases. CB-3 shows only one rate constant for its interaction with liposomes, which increases as β increases, again consistent with earlier results (Fig. 6, *d* and *e*). Because the time constant for CB-3 is much longer than the initial time constant for CB and CB-1, this suggests that CB-3 does not associate with the membrane in the manner proposed for the first stage for the cationic peptides (consistent with its lack of binding to the membranes (Fig. 4). Instead, these data are supportive of the carpet-like layer of peptides (12, 13) being the means by which CB-3 destroys membranes. The kinetic rates determined here for all three peptides are in the region of seconds, whereas those determined by Ladokhin *et al.* (42) for the indolicidin-induced leakage of 8-aminonapthalene-1,3,6 trisulfonic acid and *p*-xylene-*bis*-pyridinium bromide from palmitoyloleoylphosphatidylcholine and palmitoyloleoylphosphatidylglycerol vesicles are of the order of tens of minutes. This may be because indolicidin lacks secondary structure.

A further study of the interaction of the peptides with liposomes (at $\beta = 0.25$) was undertaken by stopped-flow CD to monitor the secondary structure of the peptides during membrane lysis. This revealed only one rate constant for the interaction of all of the peptides with the membrane and showed that the helical structure formed early in the interaction and was maintained throughout the process of membrane lysis. CB-1 had the fastest rate constant, followed by CB, with CB-3 markedly slower. This suggests that the stronger binding of the cationic peptides to the anionic membranes assists in the initial formation of secondary structure. In the case of the hydrophobic CB-3, the peptides have more difficulty associating with the membrane and so are slower to form a helical structure.

The results presented in this work suggest a mechanism for the interaction of the peptides with liposomes, leading to membrane destruction. CB and CB-1, both of which have cationic properties, associate rapidly with the membrane in an initial reaction that disturbs the membrane. This is suggested by the DL caused during this initial phase (Fig. 8). A slower, second phase occurs as the peptides interact more strongly with the lipids, possibly forming pores and effectively lysing the membrane. CB-3 shows only one step in its interaction with the peptide which is considerably slower than the first stage of the reaction of CB and CB-1 with the membranes. In this case it seems probable that the peptides will accumulate on the nonacidic parts of the membranes, destabilizing them and then, by their strong interaction with lipid tails, cause membrane lysis.

Conclusion—By using liposomes of varying acidity and peptides with differing arrangements of amphipathic and hydrophobic segments, several aspects of the interaction of cecropin peptides and liposomes have been elucidated. Although peptides with a greater cationic content bind more effectively to liposomes of increasing acidity, as shown by biosensor measurements, their efficiency at lysing these liposomes, as shown by DL measurements, decreases while the efficacy of hydrophobic peptides is increased on acidic liposomes. This shows that the high affinity binding of the peptides to the liposomes is not necessary for liposome lysis. As binding affinity increases, the cationic peptides might be inhibited from penetrating the lipid bilayer to initiate liposome lysis, whereas hydrophobic peptides might be assisted to accumulate on the reduced neutral regions of the more acidic liposomes and then disrupt the membrane. Kinetic studies showed that although helix formation for all peptides is a one-step process, the process of liposome lysis is a two-step process for the cationic peptides and a one-step process for hydrophobic peptides. These results raise the possibility that cationic peptides may act by a pore-forming mechanism, whereas hydrophobic peptides are more likely to act by a carpet-like effect.

Acknowledgments—We are indebted to Profs. Jerry Wang and Dennis Hsieh for fruitful discussions and to Drs. Reinhard Renneberg and Kevin A. W. Lee for providing the biosensor instruments. We also give many thanks to anonymous referees who provided valuable suggestions to improve the manuscript. We acknowledge the Material Characterization and Preparation Facility of HKUST for carrying out the transmission electron microscopy.

REFERENCES

1. Zasloff, M. (1987) *Proc. Natl. Acad. Sci. U. S. A.* **84,** 5449–5453
2. Ganz, T., Selsted, M. E., and Lehrer, R. I. (1990) *Eur. J. Haematol.* **44,** 1–8
3. Steiner, H., Hultmark, D., Engstrom, A., Bennich, H., and Boman, H. G. (1981) *Nature* **292,** 246–248
4. Boman, H. G. (1995) *Annu. Rev. Immunol.* **13,** 61–92
5. Cruciani, R. A., Barker, J. L., Zasloff, M., Chen, H.-C., and Colamonici, O. (1991) *Proc. Natl. Acad. Sci. U. S. A.* **88,** 3792–3796
6. Javadpour, M. M., Juban, M. M., Lo, W.-C. J., Bishop, S. M., Alberty, J. B., Cowell, S. M., Becker, C. L., and McLaughlin, M. L. (1996) *J. Med. Chem.* **39,** 3107–3113
7. Javadpour, M. M., and Barkley, M. D. (1997) *Biochemistry* **36,** 9540–9549
8. Jaynes, J. M., Julian, G. R., Jeffers, G. W., White, K. L., and Enright, F. M. (1989) *Peptide Res.* **2,** 157–160
9. Lichtenstein, A. (1991) *J. Clin. Invest.* **88,** 93–100
10. Lehrer, R. I., Lichtenstein, A. K., and Ganz, T. (1993*) Annu. Rev. Immunol.* **11,** 105–128
11. Merrifield, R. B., Merrifield, E. L., Juvvadi, P., Andreu, D., and Boman, H. G. (1994) in *Antimicrobial Peptides Ciba Foundation Symposium 186* (Marsh, J., and Goode, J. A., eds) pp. 5–20, Wiley, Chichester, U. K.
12. Gazit, E., Boman, A., Boman, H. G., and Shai, L. (1995) *Biochemistry* **34,** 11479–11488
13. Pouny, Y., Rapaport, D., Mor, A., Nicolas, P., and Shai, Y. (1992) *Biochemistry* **31,** 12416–12423
14. Christensen, B., Fink, J., Merrifield, R. B., and Mauzerall, D. (1988) *Proc. Natl. Acad. Sci. U. S. A.* **85,** 5072–5076
15. Vaz-Gomes, A., de Waal, A., Berden, J. A., and Westerhoff, H. V. (1993) *Biochemistry* **32,** 5365–5372
16. Silvestro, L., Gupta, K., Weiser, J. N., and Axelsen, P. H. (1997) *Biochemistry* **36,** 11452–11460
17. Wimley, W. C., Selsted, M. E., and White, S. H. (1994) *Protein Sci.* **3,** 1362–1373
18. Ladokhin, A. S., Selsted, M. E., and White, S. H. (1997) *Biophys. J.* **72,** 1762–1766
19. Steiner, H., Andreu, D., and Merrifield, R. B. (1988*) Biochim. Biophys. Acta* **939,** 260–266
20. Sekignchi, M., and Suzuki, T. (1994) in *Atlas of Human Tumor Cell Line* (Hay, R. T., Park, J.-G., and Gazdar, A., eds) p. 300, Academic Press, San Diego
21. Van-Blitterswijk, W. J., De-Veer, G., Krol, J. H., and Emmelot, P. (1982) *Biochim. Biophys. Acta* **688,** 495–504
22. Wiese, A., Brandenburg, K., Lindner, B., Schromm, A. B., Carroll, S. F., Rietschel, E. T., and Seydel, U. (1997) *Biochemistry* **36,** 10301–10310
23. Kim, J., Mosior, M., Chung, L. A., Wu, H., and McLaughlin, S. (1991) *Biophys. J.* **60,** 135–148
24. Ben-Tal, N., Honig, B., Peitzsch, R. M., Denisov, G., and McLaughlin, S. (1997) *Biophys. J.* **71,** 561–575
25. Ben-Tal, N., Honig, B., Miller, C., and McLaughlin, S. (1997) *Biophys. J.* **73,** 1717–1727

26. Ben-Tal, N., and Honig, B. (1997) *Biophys. J.* **71,** 3046–3050
27. Hristova, K., Selsted, M. E., and White, S. H. (1997) *J. Biol. Chem.* **272,** 24224–24233
28. Hultmark, D., Engstrom, A., Bennich, H., Kapur, R., and Boman, H. G. (1982) *Eur. J. Biochem.* **127,** 207–217
29. Fink, J., Boman, A., Boman, H. G., and Merrifield, R. B. (1989*) Int. J. Peptide Protein Res.* **33,** 412–421
30. Boman, H. G. (1991) *Cell* **65,** 205–207
31. Moore, A. J., Beazley, W. D., Bibby, M. C., and Devine, D. A. (1996*) J. Antimicrob. Chemother.* **37,** 1077–1089
32. Chen, H. M., Wang, W., Smith, D., and Chan, S. C. (1997) *Biochim. Biophys. Acta* **1336,** 171–179
33. Holak, T. A., Engstrom, A., Kraulis, P. J., Lindeberg, G., Bennich, H., Jones, T. A., Gronenborn, A. M., and Clore, G. M. (1988) *Biochemistry* **27,** 7620–7629
34. Iwai, H., Nakajima, Y., Natori, S., Arata, Y., and Shimada, I. (1993) *Eur. J. Biochem.* **217,** 639–644
35. Sipos, D., Andersson, M., and Ehrenberg, A. (1992) *Eur. J. Biochem.* **209,** 163–169
36. Mancheno, J. M., Onaderra, M., del Pozo, A. M., Diaz-Achirica, P., Andreu, D., Rivas, L., and Gavilanes, J. G. (1996) *Biochemistry* **35,** 9892–9899
37. Barlett, G. R. (1959) *J. Biol. Chem.* **234,** 466–468
38. Chang, C. T., Wu, C.-S., and Yang, J. T. (1978) *Anal. Biochem.* **91,** 13–31
39. Masson, L., Mazza, A., and Brousseau, R. (1994) *Anal. Biochem.* **218,** 405–412
40. MacKenzie, C. R., Hirama, T., Lee, K. K., Altman, E., and Young, N. M. (1997) *J. Biol. Chem.* **272,** 5533–5538
41. Lakowicz, J. R. (1983) *Principles of Fluorescence Spectroscopy*, Plenum Press, New York
42. Ladokhin, A. S., Seisted, M. E., and White, S. H. (1997) *Biophys. J.* **72,** 794–805
43. Marquardt, D. W. (1963) *J. Soc. Ind. Appl. Math.* **11,** 431–441
44. Chen, H. M., You, J. L., Markin, V. S., and Tsong, T. Y. (1991) *J. Mol. Biol.* **220,** 771–778
45. Wimley, W. C., and White, S. H. (1996) *Nature Struct. Biol.* **3,** 842–848
46. Honig, B., and Nicholls, A. (1995) *Science* **268,** 1144–1149
47. Durell, S. R., Ragunathan, G., and Guy, R. H. (1992) *Biophys. J.* **63,** 1623–1631